Lawrence Berkeley National Laboratory
Climate & Ecosystems

Title
Sixteen hundred years of increasing tree cover prior to modern deforestation in Southern Amazon and Central Brazilian savannas

Permalink
https://escholarship.org/uc/item/7dk9363x

Journal
Global Change Biology, 27(1)

ISSN
1354-1013

Authors
Wright, Jamie L
Bomfim, Barbara
Wong, Corrine I
et al.

Publication Date
2021

DOI
10.1111/gcb.15382

Peer reviewed

PRIMARY RESEARCH ARTICLE

Global Change Biology WILEY

Sixteen hundred years of increasing tree cover prior to modern deforestation in Southern Amazon and Central Brazilian savannas

Jamie L. Wright[1] | Barbara Bomfim[1,2] | Corrine I. Wong[3] | Ben H. Marimon-Júnior[4] |
Beatriz S. Marimon[4] | Lucas C. R. Silva[1,5]

[1]Environmental Studies Program, Institute of Ecology & Evolution, University of Oregon, Eugene, OR, USA

[2]Climate and Ecosystem Sciences Division, Lawrence Berkeley National Laboratory, Berkeley, CA, USA

[3]Department of Geological Sciences, University of Texas, Austin, TX, USA

[4]Laboratório de Ecologia Vegetal, State University of Mato Grosso, Nova Xavantina, Brazil

[5]Department of Geography, University of Oregon, Eugene, OR, USA

Correspondence
Lucas C. R. Silva, Environmental Studies Program, Department of Geography, Institute of Ecology & Evolution, University of Oregon, Eugene, OR, USA.
Email: lsilva7@uoregon.edu

Abstract

Tropical ecosystems are under increasing pressure from land-use change and deforestation. Changes in tropical forest cover are expected to affect carbon and water cycling with important implications for climatic stability at global scales. A major roadblock for predicting how tropical deforestation affects climate is the lack of baseline conditions (i.e., prior to human disturbance) of forest–savanna dynamics. To address this limitation, we developed a long-term analysis of forest and savanna distribution across the Amazon–Cerrado transition of central Brazil. We used soil organic carbon isotope ratios as a proxy for changes in woody vegetation cover over time in response to fluctuations in precipitation inferred from speleothem oxygen and strontium stable isotope records. Based on stable isotope signatures and radiocarbon activity of organic matter in soil profiles, we quantified the magnitude and direction of changes in forest and savanna ecosystem cover. Using changes in tree cover measured in 83 different locations for forests and savannas, we developed interpolation maps to assess the coherence of regional changes in vegetation. Our analysis reveals a broad pattern of woody vegetation expansion into savannas and densification within forests and savannas for at least the past ~1,600 years. The rates of vegetation change varied significantly among sampling locations possibly due to variation in local environmental factors that constrain primary productivity. The few instances in which tree cover declined (7.7% of all sampled profiles) were associated with savannas under dry conditions. Our results suggest a regional increase in moisture and expansion of woody vegetation prior to modern deforestation, which could help inform conservation and management efforts for climate change mitigation. We discuss the possible mechanisms driving forest expansion and densification of savannas directly (i.e., increasing precipitation) and indirectly (e.g., decreasing disturbance) and suggest future research directions that have the potential to improve climate and ecosystem models.

KEYWORDS
carbon, climatic change, forest–savanna dynamics, stable isotopes, woody expansion

1 | INTRODUCTION

Over the previous decade more than 200 million hectares of forested land was deforested in the tropics (Austin et al., 2017) with approximately 40% of that deforestation occurring in Brazil's Amazon and Cerrado ecoregions (Levy et al., 2018). Earth system models suggest that tropical forest cover loss of this magnitude, if continued, will alter water and carbon cycles and climatic patterns (Garcia et al., 2016). For instance, atmospheric moisture increases significantly with forest cover due to tree transpiration, a process that favors continuous rainfall recycling (Spracklen et al., 2012), and buffers drought impacts regionally (Staal et al., 2018). Although this forest–atmosphere feedback can be used to predict linkages between changes in primary productivity and tree cover, and between tree cover and precipitation (Sternberg, 2001), many uncertainties surround the past and future of tropical ecosystems as a stabilizing climatic force. These uncertainties are, at least in part, rooted in a lack of empirical data to parameterize scenarios before and after deforestation became a dominant planetary force (Silva & Lambers, 2018). In this study, we address some of these uncertainties by measuring proxies to estimate long-term changes in forest–savanna distributions and carbon–water relations in a region of global significance, the Amazon–Cerrado transition of central Brazil.

The Amazon–Cerrado transition spans a broad climatic and ecological gradient, with tree cover increasing as moisture increases from seasonally dry savanna-dominated landscapes towards the Amazon monsoon core (Elias et al., 2019). At one end of the transition, Amazon rainforests dominate under the influence of the South American summer monsoon (SASM). At the other end of the transition, under more seasonal precipitation, different types of ecosystems coexist including grasslands, savannas, and forests. Throughout the region, vast areas of relatively undisturbed vegetation (i.e., mostly protected from direct human impact until very recently; Freitas et al., 2018) allow for the study of connections between climate variability and ecosystem processes, such as water use and carbon accumulation in biomass and soils. For example, sharp forest–savanna ecotones (i.e., boundaries within a few meters), which are commonly found in the region, have been shown to shift with long-term changes in precipitation (Silva et al., 2008). At local scales, such sharp ecotones are also maintained by fires, which occur regularly in savannas but do not typically penetrate into dense forests (Hoffmann et al., 2012). At regional scales, fire frequency and intensity are influenced by precipitation. Thus, if sufficiently widespread, changes in precipitation can cause biome scale rearrangements as well as incremental expansion of tree cover outward from local forest–savanna transitions.

Due to high primary production, the expansion of woody vegetation in savannas can significantly increase carbon stocks aboveground and belowground (Abreu et al., 2017; Duarte-guardia et al., 2019; Silva, 2017). However, this is not always the case because many savanna species tend to invest a significantly greater portion of their net carbon gain toward belowground biomass (Miranda et al., 2014; Veldman et al., 2015). Beyond carbon sequestration,

increasing tree cover in forests and savannas can increase precipitation due to increased transpiration (Spracklen et al., 2012; Zemp et al., 2017). Therefore, understanding long-term changes in tree cover is critical for understanding the future of essential ecosystem carbon and water cycling functions, as well as the role of those ecosystems in supporting high levels of biodiversity and endemism that characterize the region (Abreu et al., 2017; Brannstrom et al., 2008).

Previous studies have found a trend of forest expansion into savannas in Brazil since the mid-Holocene, which has been interpreted as an indication of increased precipitation (Silva, 2014; Silva et al., 2008). Those studies were performed using a few strategically selected sites which indicated that tree cover increased near riparian forest margins as well as in some upland savannas. However, it remains unclear if this expansion of woody vegetation was a localized phenomenon or if it represents a broader process caused by climate dynamics throughout the region. To answer this question, we reconstructed forest and savanna tree cover across paleolandscapes using radiocarbon (^{14}C) dating and stable carbon isotope signatures (δ^{13}C) of soil organic matter (SOM). This approach is based on two assumptions: (a) that the average age of SOM increases with depth through the soil profile, such that each profile represents a chronological sequence of vegetation inputs (Schmidt et al., 2011; Trumbore, 2000); and (b) that differences in stable carbon isotope ratios between savanna and forest biomass occur due to marked differences in the relative abundances of trees and grasses and lead to unequivocal SOM isotope signatures from either ecosystem (von Fischer et al., 2008; Victoria et al., 1995). Based on these assumptions we moved beyond local reconstructions to generate current and paleo data from 83 different sites, which allowed us to develop regional maps that relate SOM isotope signatures and spatial changes in ecosystem cover through time.

2 | MATERIALS AND METHODS

2.1 | Study region

Our study region spans latitudinally from Pará State to Goiás State (4°S–16°S) and longitudinally from eastern Tocantins State to central Mato Grosso State (46°W–56°W) in Brazil (Figure 1). Annual precipitation ranges from 1,250 to 2,500 mm, with precipitation amounts and distribution varying significantly across the study region (Figure 1a). Eastern and southern sites are characterized by strong seasonality (i.e., wet summers and dry winters) whereas more constant precipitation inputs persist near the monsoon core, at the northern and western sites (Ward et al., 2019). A less important temperature gradient exists throughout the study region with respect to the precipitation gradient, in which mean annual temperature ranges from 22 to 26°C (Figure 1b). Across the region we gathered vegetation and soil data from 46 forests, 26 savannas, and 10 transitions (i.e., sites classified as forest–savanna ecotones) from a combination of published (Silva et al., 2008, 2010) and new sampling locations (Table S1). Soil taxonomy was determined at order level using the Brazilian soil classification system
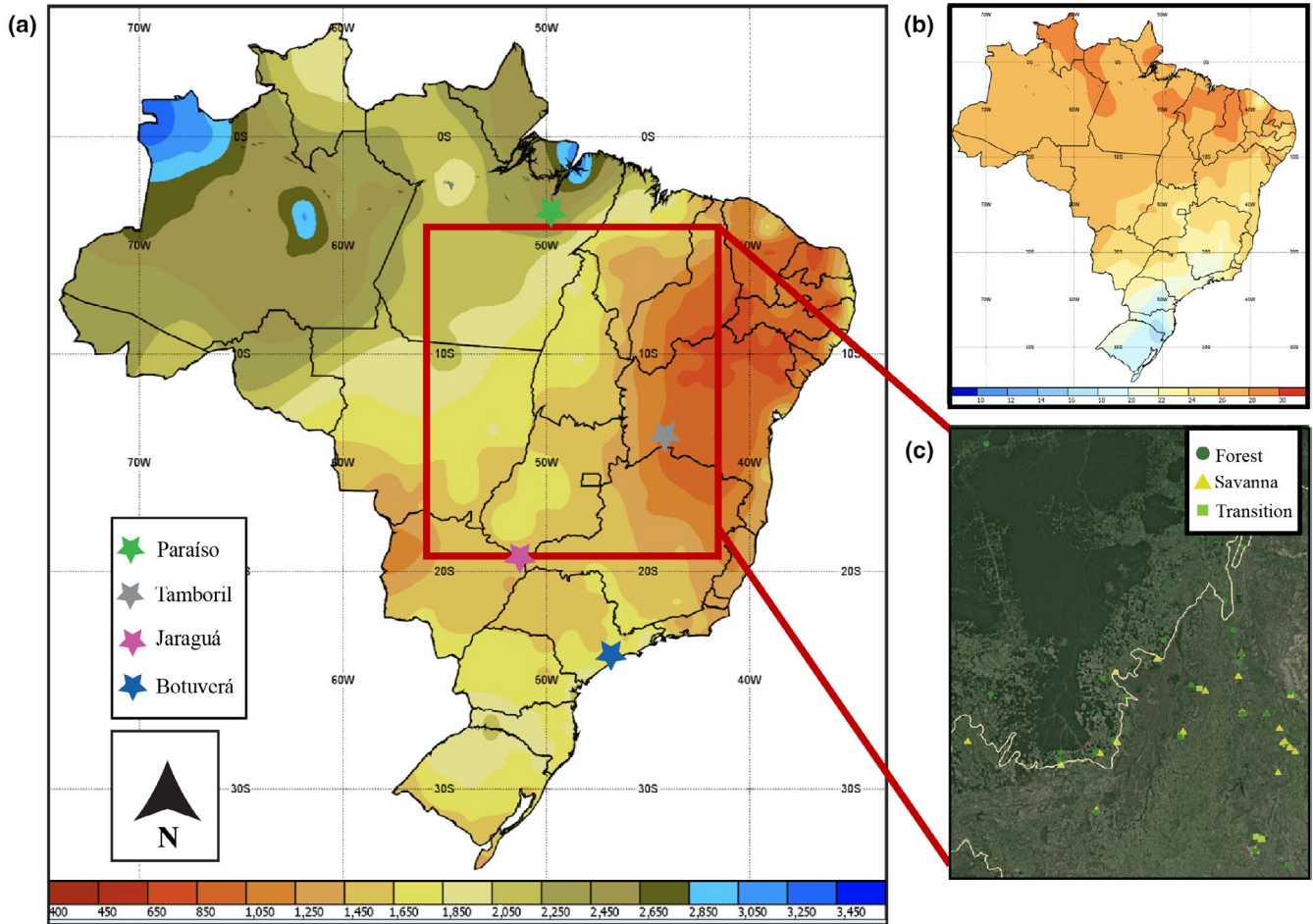
FIGURE 1 Study sites, current ecosystems, and climate: (a) mean annual precipitation (mm) over the time period 1981–2010. Blue stars indicate cave sites where paleoclimate records were derived from speleothems. (b) Mean annual temperature (°C) over the time period 1981–2010. (c) Study region displaying 83 sites sampled for this study within the Amazon–Cerrado region. The yellow line within the study region delineates the ecoregions—Amazon to the Northwest and Cerrado to the Southeast. Shapes and colors correspond to forest, savanna, or forest–savanna transitions. Climate map adapted from INMET (2019)

and converted to the nearest matches in the USDA system (Soil Survey Staff, 2014). We controlled for recent changes in land use and vegetation cover when choosing sampling sites. First, we excluded sites that displayed distinct signs of human disturbance (e.g., deforestation, non-native species, or grazing). Second, we relied on local expert collaborators to identify and exclude any sites where the floristic composition and vegetation structure could not be classified as typical of native forests and savannas. Finally, all selected sampling locations correspond to legally protected public or private land where forests and savannas appeared to be at steady conditions, with no major changes in vegetation cover or land conversion, detectable in ~20 years of satellite images (AppEEARS Team, 2019; Didan, 2015).

2.2 | Ecosystem cover

To characterize ecosystem cover we measured leaf area index (LAI) in forests and savannas throughout the region using a combination of standard ground-based and satellite-based measurements (Ladd et al., 2013). A negative relationship between current LAI and $\delta^{13}C_{SOM}$ is to be expected because trees and other C_3 woody plants discriminate more against the heavier ^{13}C carbon isotope relative to ^{12}C than do C_4 grasses (Smith & Smith, 2015), which dominate in this region and give rise to unequivocally distinct $\delta^{13}C_{SOM}$ signatures. Previous research has found a significant linear relationship between topsoil $\delta^{13}C_{SOM}$ values and LAI (Ladd et al., 2014), which allows for reconstructing past tree canopy cover using deep $\delta^{13}C_{SOM}$ signatures. Although input and decomposition rates vary significantly with ecosystem type, as well as soil properties and microbial community composition, there is no overlap between SOM carbon isotope signatures from tree- and grass-dominated systems in our region (Ladd et al., 2014). Here, we build on that finding by adding 83 new sites to improve the quantitative inference of tree cover from $\delta^{13}C_{SOM}$ values. Our data confirm expectations and show a significant decline in $\delta^{13}C_{SOM}$ with increasing LAI measured using ground-based measurements and Moderate Resolution Imaging Spectroradiometer (MODIS)

15A2 and MCD15A3H (https://doi.org/10.5067/MODIS/MCD15 A3H.006; Appendix 1).

Ground-based LAI measurements were taken with a 180° hemispherical lens to estimate total tree cover per area of ground cover across all vegetation types captured from approximately 1 m above the soil surface at forested sites, which typically lack grass cover, and at approximately 1 m height and at the soil surface for savanna sites to incorporate grass cover. Ground-based LAI calculations were done using the open source Gap Light Analyzer software (Frazer et al., 1999), where the blue color plane was used as a threshold to better distinguish between sky and vegetation. The LAI estimates obtained in this way represent total tree cover rather than green leaf area per se, such that our values of LAI include stem area, as well as leaf area. In forests, C_4 grasses are non-existent, but when tree cover declines C_4 grasses dominate open ecosystems, therefore, the resulting relationship between ground- and MODIS-derived LAI is unambiguous ($R^2 = .91$; $p < .0001$) and tree cover can be inferred from SOM carbon isotope ratios (Figure 2). Spatiotemporal changes in tree cover can then be visualized using point data interpolation from individual sites and profile depths (Kahle & Wickham, 2013) assuming certain conditions for organic carbon inputs and permanence, which are described as follows.

2.3 | Soil sampling

Soil samples were collected from forest ($n = 46$), savanna ($n = 26$), and forest–savanna transition zone ($n = 10$) ecosystems. At each site, up to five soil profiles were collected near the LAI measuring location (when measured with ground-based technique). The regions with fewer sample sites are within the Amazon ecoregion where forests have persisted since at least the mid-Holocene (Smith

& Mayle, 2018). The exact location and number of profiles sampled at each site are shown in Table S1. The majority of soil profiles extended to a depth of approximately 100 cm. At some sites, we were capable of sampling down to 200 cm depth. At few locations, shallower profiles were collected where the bedrock was reached before a 100 cm depth. Soil samples were retrieved in 5–10 cm increments, sieved, air-dried and homogenized by depth of collection within each site. This effort resulted in 742 individual samples which were subsequently prepared for analysis of total organic carbon content and stable isotope ratios. A representative number of samples were selected for determination of radiocarbon activity as follows.

2.4 | Soil carbon: Age-depth model and vegetation reconstruction

To determine changes in ecosystem cover, we used stable carbon isotope signatures ($\delta^{13}C_{SOM}$ given in permille [‰] units), which compare the proportion of ^{13}C to ^{12}C in SOM of each sample relative to an internationally accepted standard (Vienna PeeDee Belemnite). For this analysis, bulk SOM samples of all 742 individual samples were ground and homogenized after the removal of undecomposed plant material, powdered using an automated ball mill and manually encapsulated in 5×8 mm tin capsules (sample size approximately 0.25–0.70 mg). Isotopic ratios were determined by dry combustion gas chromatography coupled with continuous-flow isotopic-ratio mass spectrometry (GC-IRMS 20-20/ANCA-NT; Europa, at the University of California, Davis Stable Isotope Facility), measured with expected $SD < 0.2$‰. Carbon content per sample was calculated to optimize aliquot amounts for radiocarbon dating. Soil samples were prepared following standard procedures, air-dried and passed through a 2 mm sieve in which aliquots were ground using a ball mill in preparation
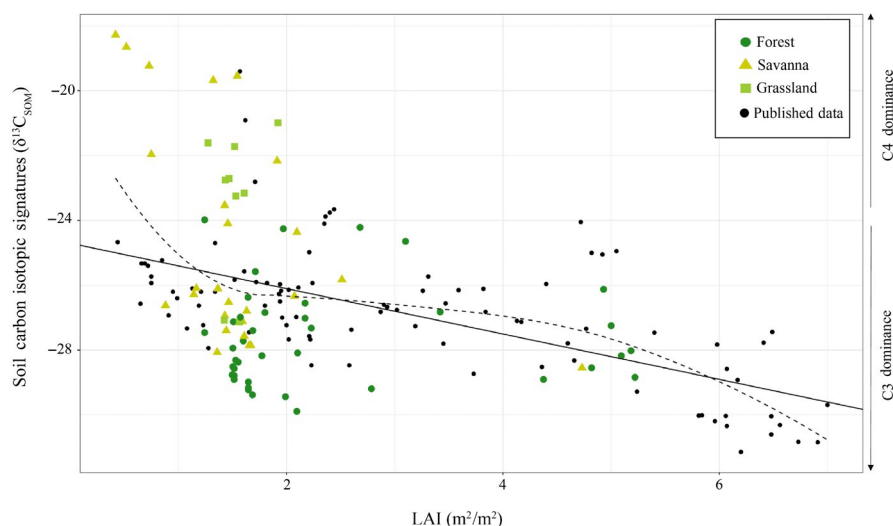

FIGURE 2 Relationship between topsoil soil organic matter carbon isotope signatures ($\delta^{13}C_{SOM}$) and ground-based or satellite-derived leaf area index (LAI; Table S2). Less negative $\delta^{13}C_{SOM}$ values correspond to C_4 grass dominance. More negative $\delta^{13}C_{SOM}$ values correspond to C_3 woody vegetation dominance. Shapes and colors correspond to current ecosystem type. The black line displays a significant linear regression between $\delta^{13}C_{SOM}$ and LAI ($R^2 = .23$; $p < .0001$). The dashed black line displays non-linear regression between $\delta^{13}C_{SOM}$ and LAI ($R^2 = .30$). Previously published data (represented by black points) adapted from Ladd et al. (2014)

for δ^{13}C analysis and ^{14}C dating. Approximately 800 mg of bulk soil was sent to the University of California, Irvine Keck Carbon Cycle Accelerator Mass Spectrometer Facility, where a precision of ~1% on samples with 100 μg or more of carbon is routinely achieved.

To determine changes over time, we measured radiocarbon (^{14}C) activity in 43 strategically selected depths from soil profiles sampled in forests ($n = 20$), savannas ($n = 11$), and forest–savanna transitions ($n = 12$) considered representative of each ecosystem and soil type. This effort resulted in calibrated radiocarbon dates for profiles sampled in about one third of all sampled sites (26 out of 83). Only a few sites were suspected of containing carbonates (three out of 83) based on pH, a one-way ANOVA showed no significant difference ($p = .83$) between acid treated and non-treated δ[13]C_{SOM} aliquots of those samples. We found that three riparian sites (likely seasonally flooded) had current SOM ^{14}C signatures at deep layers (≥80 cm). Those sites were removed from the analysis. No statistical differences were found on the basis of soil type ($p > .05$) using an ANCOVA test. We used the same test for ecosystem types and found that only forest–savanna transitions possessed statistically different regression slopes from other ecosystems. Therefore, we chose to use a single regression including forests and savannas even though we found high site-specific variation around the age-depth mean (as shown in the Figure 3). Consequently, the average age of vegetation change reported here should be understood as a regional approximation rather than a precise date for shifts within sites, which require local analysis and interpretation as each site. A linear age-depth regression explains most of the variance in SOM age across sites ($R^2 = .73$; $p < .0001$; Figure 3). The vast majority of soil profiles surveyed extended to at least 80 cm depth and yielded

sufficient SOM for isotopic analysis (Figure 4). For this reason, 80 cm was used as the reference depth/age for comparison of past vegetation cover across the region (Figure 5). At the selected depth, the average age across sites is 1,595 years before present and the SEM is 404 years (Figure 3), hereafter referred to as ~1,600 years for simplicity.

The results reported here represent isotopic ratios and radiocarbon activities of organic carbon pools. To ensure that inorganic carbon was not included in the analysis, soil pH was measured in samples suspected of possessing carbonates, which are rare in Oxisols but common in some dolomite outcrops near the north-easternmost sites (Silva et al., 2010). Potential presence of carbonates (pH > 5) was identified for three sites (Site 79, 81, 82; Table S1). Samples from those sites were treated with hydrochloric acid (HCl) and resubmitted for analysis of radiocarbon and stable isotope ratios. The samples were subsequently put into an oven until the HCl solution evaporated. The samples were repeatedly washed with deionized water to bring the pH above 4.0. Some samples were centrifuged to separate fine particles from solution in order to minimize sample loss. The samples for carbon stable isotope analysis were treated with 1 M HCl to remove carbonates. Two milliliters of the 1 M HCl solution was added to each sample of approximately 0.25–0.70 mg in a glass vile, in which samples were placed in an oven until the HCl solution evaporated. To determine if there was a significant difference between acid treated and non-treated soil samples for stable isotope analysis (δ[13]C_{SOM} values), a one-way ANOVA was performed. Two standards were acid-washed using the same procedure applied to soil samples. The standards included a modern and a "dead" sample in which the modern sample came from deciduous tree leaves and the dead was anthracite coal. These standards were used to make background corrections when analyzing soil samples' ages (Santos et al., 2019). The samples for radiocarbon dating were treated with 0.1 M HCl.
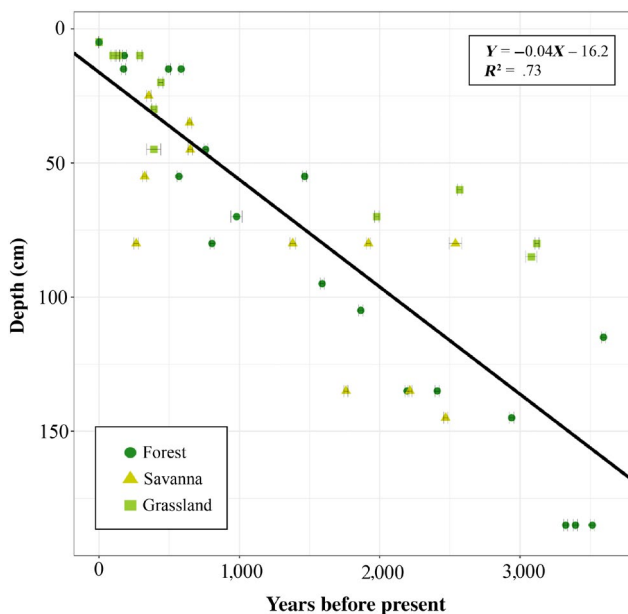
2.5 | Spatial interpolation and regional analysis

To reconstruct paleolandscapes across the study region, interpolation maps were generated using ordinary kriging, as in previous geostatistical studies of soil data (e.g., Elbasiouny,et al., 2014; von Fischer et al., 2008). This approach allows predictions of unknown spatial data to be determined with minimum variance and removed bias under the following assumptions: variation in the data is random and stationary (Oliver & Webster, 2014). The method fits a variogram model to the data, in which a variogram is the semivariance as a function of the data's direction and distance separation. The only input data was δ[13]C_{SOM} with their corresponding coordinates. Since no other variable was interpolated, ordinary kriging was used instead of alternative kriging methods.

Maps were first made for the current environment using topsoil data (0–10 cm), intermediate layers (i.e., 30, 50, 70 cm) and down to a depth of 80 cm. Then a change "heat map" for its difference relative to current conditions was developed (i.e., topsoil minus 80 cm layer). We used a depth of 80 cm for two reasons. First, on the basis of δ[13]C_{SOM}

FIGURE 3 Age-depth model displaying relationship between soil depth and calibrated radiocarbon years before present. Ecosystem type (i.e. forest, savanna, transition) are distinguished using different colors and shapes in which standard deviations represent analytical uncertainty
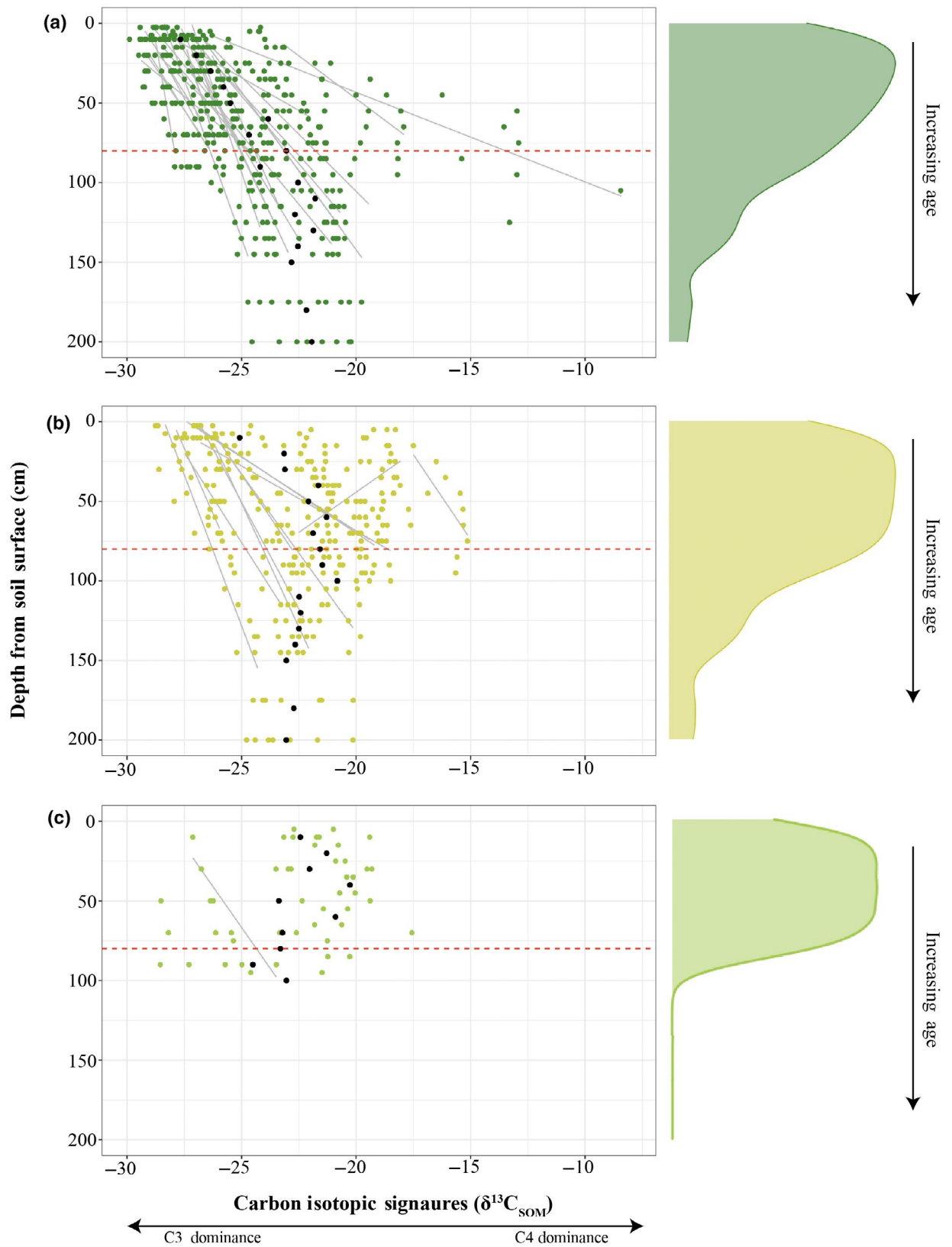
FIGURE 4 Soil organic matter carbon isotope ratios ($\delta^{13}C_{SOM}$) across depths for (a) forest, (b) savanna, and (c) forest–savanna transitions. Figures to the right show the proportion of data points for each soil depth. Grey lines represent significant linear regressions ($p < .05$) between soil depth and $\delta^{13}C_{SOM}$ within each soil profile. Red-dashed lines indicate the depth of 80 cm selected for vegetation reconstructions across all sites. Black points represent averages per depth. The majority of regressions indicate increasing woody cover over time
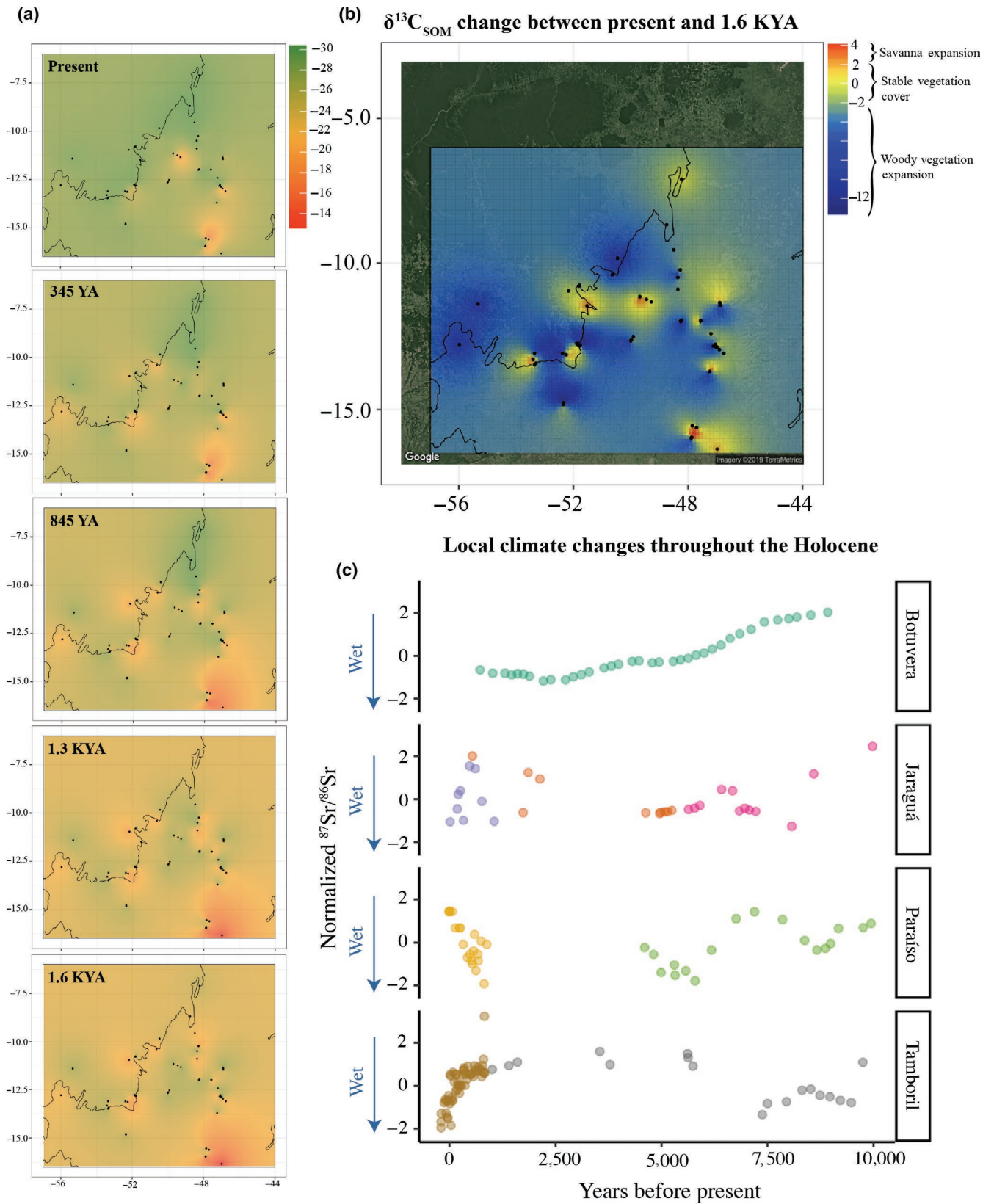
FIGURE 5 Changes in δ¹³C$_{SOM}$ at (a) varying depths across study sites, where the *x*-axis is longitude and the *y*-axis is latitude, and depth has been converted to age; (b) vegetation change heatmap where blue represents woody vegetation expansion, yellow represents no change, and red represents grass expansion; and (c) strontium isotope ratios, adapted from Ward et al. (2019), as a proxy for soil moisture and rock dissolution, indicating a shift towards wetter conditions. Different colors within each location represent different speleothem samples collected within the same cave site (Figure 1)

signatures it was apparent that significant changes in vegetation cover happened across most sites at age corresponding to that depth (i.e., ~1,600 years ago). Second, the majority of sites had profiles that would go to that depth or beyond. The heat map of change was generated by subtracting the intermediate layer at 80 cm from topsoil so that the direction of change would correspond with forest or savanna $\delta^{13}C_{SOM}$ signatures (i.e., negative values represent increasing tree cover and positive values indicate decreasing tree cover). Averages were used when sites had multiple samples from the same depth interval. One of the study sites (Site 56, Table S1) located deep within the Amazon was removed when generating the interpolation maps due to its distance from other clustered sites, which decreased the robustness of the interpolation maps. Notably, that site has been relatively "stable" meaning that its $\delta^{13}C_{SOM}$ profile signatures have been that of a dense forest for the past several thousand years which does not affect our analysis of change in tree cover at other locations since ~1,600 years ago.

In some regions of our interpolation map, fewer data points exist and the spatial variance increases in those regions, but tree cover increased in the vast majority of sites regardless of variance within and across ecosystem. To evaluate the robustness of the underlying variogram we used goodness-of-fit analysis for each kriging map applying different common variograms (i.e., exponential, spherical, Gaussian). To quantify goodness-of-fit, each models' root mean square error (RMSE) values were quantified after performing cross-validation on each model type. The variogram model that fit the data the best was the exponential model based on cross-validation and RMSE values (2.8, 3.4, 3.6 for topsoil, intermediate, and change layer). For simplicity, we only present the best models selected through this approach. A one-way ANOVA was run between the observed and fitted groups generated from kriging, displaying that the observed and fitted values were not statistically different ($p = .90, .39, .43$), consequently indicating that the ordinary kriging model fits our data.

To investigate whether climate (regional and local) matched tree cover we used previously reported oxygen (Ward et al., 2019) and strontium (Wortham et al., 2017) data from speleothems. Oxygen data were collected throughout Brazil, as observed in figure 1 of Ward et al. (2019) and strontium data locations are shown in Figure 1, denoted by blue stars. Oxygen isotope ratios ($\delta^{18}O$) reflect regional SASM intensity and strontium isotope ratios ($^{87}Sr/^{86}Sr$) reflect soil moisture and rock dissolution (Ward et al., 2019; Wortam et al., 2017). Speleothem isotope ratios were normalized ($z = (x - mean)/SD$) within each site to allow for trends to be compared across sites. To better interpret the average regional change in vegetation cover over space and time, we used a mixing model (Parnell, 2020) to quantify C_3- versus C_4-derived contributions to the bulk $\delta^{13}C_{SOM}$ signatures between topsoil (10 cm) and an intermediate depth (80 cm) of known age (Figure S1). Source values for C_3 and C_4 vegetation were based on typical grassland and forest signatures measured across the region (−27‰ and −12.5‰; respectively). A Tukey honestly significant difference (HSD) test was performed to determine at what depth differences in $\delta^{13}C_{SOM}$ signatures became significant within each ecosystem relative to the topsoil (0–10 cm).

2.6 | Soil carbon: Stocks and relationship to changes in vegetation

To better understand whether and how changes in forest and savanna cover influence soil carbon stocks, we quantified soil carbon concentrations at each study site profile and soil depth. To better estimate the timing of vegetation change and its resulting effects on soil carbon stocks, bulk density (g/cm^3) from a subset of typical forest, savanna, and transition ecosystems were supplemented by radiocarbon and stable isotope datasets from previously published studies conducted in central Brazil (Silva et al., 2008, 2010, 2013). To match the analysis of ecosystem cover (described above) we report carbon stocks down to 80 cm at all sites. The relative contribution of C_3 and C_4 plants to SOM across sites is shown in Figure S1. A mixed-effects model was applied to test the significance of fixed effects (ecosystem type, soil order, and paleovegetation) as well as random effects (sampling site nested within ecosystem type) on soil carbon stocks (Figure S2). The geographic location and basic description of ecosystem and soil types at all sites are shown in Table S1. The data used to produce all figures are available at https://scholarsbank.uoregon.edu/.

3 | RESULTS

3.1 | Current ecosystem cover and $\delta^{13}C_{SOM}$

In Figure 2 we show a linear regression describing the relationship between LAI and topsoil $\delta^{13}C_{SOM}$ to be significant ($R^2 = 0.23$; $p < .0001$; error = 2.15) which is consistent with previous studies of this kind (Ladd et al., 2014). However, when we applied a non-parametric function (locally weighted regression) to our data, the relationship improved and possessed a lower model error ($R^2 = .30$; error = 2.06). In either scenario, carbon isotopic signatures become more negative (i.e., representative of increasing tree cover or woody vegetation dominance) as LAI values increase. Conversely, increasingly positive carbon isotopic signatures are found with declining LAI and dominance of herbaceous plants, which in this region means increasing dominance of C_4 grasses.

3.2 | Soil carbon: Age-depth model and vegetation reconstruction

In Figure 4 we show all $\delta^{13}C_{SOM}$ data by profile and site. The vast majority of sites show trends within profiles that indicate a gradual change in carbon isotopic signatures due to woody vegetation expansion or densification. Least square regressions are used to describe significant changes in $\delta^{13}C_{SOM}$ within each sampled profile (gray lines) in forests, savannas, and transition zones. The proportion of our sites that can be linked to changes in vegetation cover (Figure 5) is based on a four permille threshold for ecosystem stability, which excludes enrichment or depletion from diagenetic

fractionation. Based on those criteria we quantified a major shift in paleovegetation cover in which 7.7% (five) of the sites' $\delta^{13}C_{SOM}$ values became more positive (i.e., moving towards grass-dominated signatures), 24.6% (16) remained stable (less than plus or minus two permille), and 67.7% (44) became more negative (i.e., moving towards tree-dominated signatures) moving up the soil profile.

The rate of vegetation change was significantly different ($p < .001$) among ecosystem types, but the coefficient of variation for changes in vegetation within forest, savanna, and transition sites was high (74.0%, 55.0%, and 281%, respectively). Despite large variability among sites, a consistent increase is woody vegetation cover was observed for the vast majority of forest and savanna ecosystems. Figure 4a–c shows the rate of vegetation change for each soil profile down to a depth of 200 cm, in which depth averages (the black points), individual soil profile linear regressions (gray lines—if significant with a $p < .05$, are included within each plot). Depth averages per ecosystem type are included in Table S3. The proportions of C_3 and C_4 plants' contribution to SOM was calculated using a stable isotope mixing model for topsoil (current) and deep soil (70–80 cm; old) for all forest and savanna ecosystems (Figure S1). A Tukey HSD test showed that $\delta^{13}C_{SOM}$ isotopic signatures became statistically different from current values at depths ranging from 30 to 50 cm at most forests and savannas. At transition zones, current $\delta^{13}C_{SOM}$ isotopic signatures did not differ significantly from other depths. A mixed-effects model (Figure S2) including the random effect, sampling site nested within ecosystem, performed better than other models that included no random effects. The fixed effects of depth, ecosystem type and their interactions had significant effects ($p < .05$) on the response variable ($\delta^{13}C_{SOM}$). Soil order did appear to have a significant effect ($p > .05$) on $\delta^{13}C_{SOM}$, however, soil order improved the overall model when included. Model quality comparisons were derived from the Akaike information criteria in which smaller values indicate better model fit.

3.3 | Spatial interpolation and regional analysis

The $\delta^{13}C_{SOM}$ kriging maps for topsoil (0–10 cm), intermediate layers, and deep soil (70–80 cm), and their difference heat map between 80 cm and topsoil (Figure 5) showed that the vast majority of sites (67.7% of all sampled profiles) followed a trend of woody vegetation expansion and densification over time. The few instances in which tree cover declined (7.7% of all sampled profiles) were associated with dry conditions in savannas on rock outcrops at the easternmost sampling sites, which as shown in Figure 1, are characterized by warm and dry climate. The topsoil map (Figure 5a) represents current ecosystem cover as a function of C_3 versus C_4 abundance, with $\delta^{13}C_{SOM}$ ratios consistent with typical forest and savanna isotopic signatures (ranging from −29‰ to −18‰). The deep soil layer at 80 cm selected for mapping (Figure 5a), representing past ecosystem cover ~1,600 years ago, shows a landscape dominated by more positive $\delta^{13}C_{SOM}$ ratios (i.e., less negative values that are characteristic of savannas and grasslands) ranging from −26‰ to −13‰. The intermediate depths, which have been converted to years before present,

suggest that the trend of woody vegetation expansion and densification has been a gradual shift over time rather than an abrupt transition, which is often characteristic of anthropic interventions. Using the linear model presented in Figure 2 the observed changes in $\delta^{13}C_{SOM}$ ratios can be converted to units of LAI (Table S4). We only used our linear regression to convert $\delta^{13}C_{SOM}$ ratios to LAI, since it is consistent with previous studies (Ladd et al., 2014).

Topsoil soil $\delta^{13}C_{SOM}$ is known to reflect differences in vegetation cover across biomes, especially in tropical regions where the isotopic difference between tree- and grass-dominated system reaches its maximum value (Ladd et al., 2014). As expected, we found a significant negative relationship between LAI and current $\delta^{13}C_{SOM}$ ratios, which serve as a baseline from which past ecosystem dynamics can be retraced. The heat map of change (Figure 5b) shows the marked shifts in $\delta^{13}C_{SOM}$ raw data in which different colors indicate the magnitude and direction of vegetation change over time. Blue regions represent −13‰ to −3‰ shifts, which are indicative of changes towards woodier vegetative signatures. Whereas warmer colors (i.e., orange–red, red) represent 3‰–6‰ shifts, which indicate areas where forests have receded or been replaced with mixed grass-shrub vegetation or grasslands. The raw isotopic ratios of SOM also incorporate changes in the isotopic composition of atmospheric CO_2 due to the emission of fossil fuels over the past century (known as the Suess effect). However, changes in $\delta^{13}C$ ratios of CO_2 have been small for most of the Holocene (<1.5‰ over the past 10,000 years; Hare et al., 2018) and those changes would have affected both tree and grass biomass $\delta^{13}C$ signatures in similar ways. We can therefore rule out this predepositional process as an explanation for long-term changes in $\delta^{13}C_{SOM}$, which happened before anthropogenic CO_2 emissions became a significant planetary force. Although it is difficult to distinguish between processes that occur after SOM deposition, postdepositional changes occur primarily in the topsoil as litter decomposes, typically leading to a <2‰ fractionation (Krull et al., 2002). To be conservative, we only present interpolated $\delta^{13}C_{SOM}$ maps in which shifts greater than ±2‰ occurring at depths from 30 to 50 cm or deeper in the soil profile. As a result, the yellow to yellow-green colors in the interpolation maps indicate regions of relatively "stable" ecosystem states; that is, those in which $\delta^{13}C_{SOM}$ varied between −2‰ and 2‰ within any given profile.

Variation in the reconstructed changes in tree cover and woody vegetation expansion are consistent with local to subregional hydroclimate variability, inferred from speleothem strontium ratios which indicate increasing soil moisture and rock dissolution near most, but not all, soil sampling sites (i.e., a general shift to more negative Z-scores characteristic of wetter conditions; Figure 5c). The steepest and most consistent increase in moisture conditions, inferred from strontium isotopes, was observed for the Tamboril site in central Brazil. No clear trend in hydroclimate was observed for the Paraiso cave, suggesting stable moisture regime at our northernmost site in the Amazon region. All other cave sites showed some degree of increasing moisture with significant subregional variability, oscillating between the trends displayed in the Tamboril and Paraiso records. The regional record of monsoon intensity, inferred from speleothem
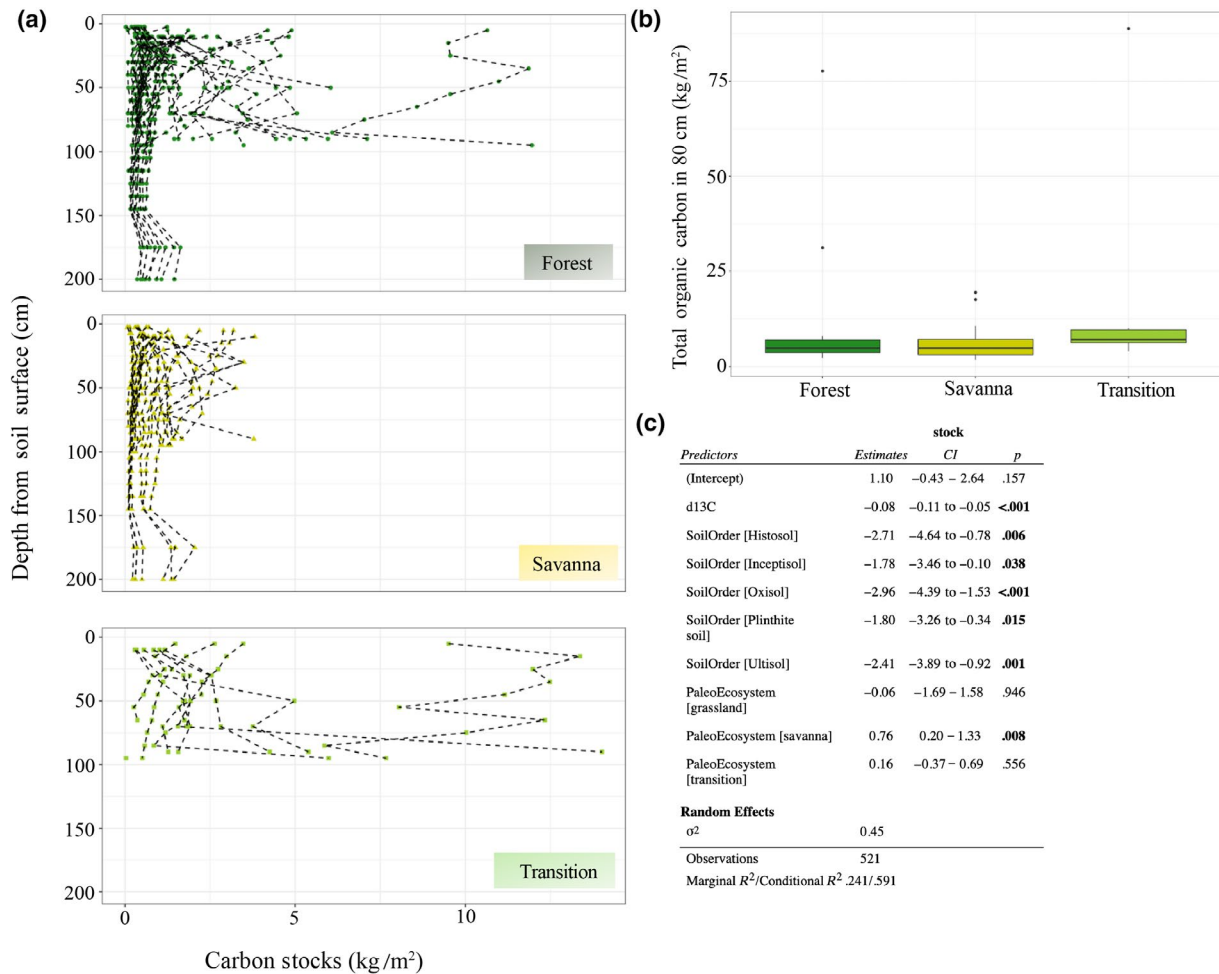
FIGURE 6 Variation in soil organic carbon stocks for each ecosystem and soil depth (a). Small differences were found for average carbon stocks across ecosystems, although notable outliers exist within forests and forest–savanna transitions (b). A mixed-effects model indicates that soil order and woody vegetation expansion significantly affected soil carbon content only in savannas, where woody vegetation expansion had a positive effect on carbon stocks, with a significant random effect of sampling location for all ecosystem types (c)

oxygen isotope ratios, showed a less consistent signal of increasing precipitation, with larger variability than the local trends in hydro-climate throughout the region for most of the Holocene (Figure S3).

3.4 | Soil carbon: Stocks and relationship to vegetation cover

Carbon stocks decreased significantly with depth ($p < .001$) as observed in Figure 6a. There was also a significant difference in carbon stocks (to a depth of 80 cm) among ecosystem types (Figure 6b). The mixed-effects model applied to carbon stocks per depth indicated that the fixed effects of paleovegetation (i.e., from ~1,600 years ago) had significant effects ($p < .05$) on carbon stocks per depth only within past savannas, where increasing tree cover had a positive effect on carbon storage. Soil type was not a significant predictor of SOM carbon isotope ratios (Figure S2), but it was a strong predictor of carbon stocks (Figure 6c), even though we found a significant random effect (sites nested within present ecosystem

type) indicating that variation in carbon stocks depended on sampling location.

4 | DISCUSSION

There have been many studies about the effects of deforestation at the Amazon–Cerrado transition, but little is known about long-term variation in tree cover and climate before modern deforestation. Here, we report evidence of a widespread process of increasing tree cover prior to modern deforestation. Our findings are supported by isotopic data which display a general trend of woody vegetation expansion and densification over at least the past 1,600 years in forest- and savanna-dominated landscapes. Overall, the spatial pattern observed amounts to a regional process of woody vegetation expansion that happened either through forest encroachment into savannas or through densification of tree cover in previously grass-dominated systems. Our data indicate an increase in precipitation during the mid- to late-Holocene transition, which is consistent

with independent climate reconstructions from lake sediment pollen and charcoal (Behling, 1998; Bird et al., 2011; Sande et al., 2019; Sternberg, 2001) and from speleothem carbonate oxygen and strontium records (Cruz et al., 2005; Vuille et al., 2012; Ward et al., 2019; Wortham et al., 2017). Specifically, our analysis of SOM across 83 study sites supports the hypothesis of increasing tree cover due to increasing moisture inferred from speleothem-based reconstructions that reflect spatial and temporal variation in climate across the region.

Regarding the timing of forest or woody savanna expansion, our SOM ^{14}C data represent the most recent changes in vegetation out of a range of possible ages. Soil develops from two directions, with mineral weathering occurring primarily in deep layers near the parent material and new organic inputs occurring primarily near the soil surface. However, current inputs can also occur within and beyond the rhizosphere (e.g., via root exudates and rhizodeposition). Given that recent addition of carbon into the deeper soil matrix can occur, calibrated ^{14}C dates of bulk organic matter represent an average age of vegetation input for any given depth. This interpretation is consistent with several previous studies, which showed a general trend of savanna systems (having a C_4 signature) being replaced with forests (having a C_3 signature) as inferred from SOM (Berhe et al., 2012; Sanaiotti et al., 2002; Trumbore, 2009). Large variance is to be expected within and across ecosystems because, although differences in molecular composition of tree- and grass-derived litter and their relative contributions to SOM are not expected to affect soil carbon stability, other environmental and biological factors can affect carbon turnover (Schmidt et al., 2011). Therefore, the estimated ~1,600 years of woody vegetation expansion should be understood as the mean minimum age of SOM associated with ecosystem change, which probably began earlier as suggested as suggested in previous case studies (e.g., Silva, 2014), triggered by mid-to-late Holocene changes in the regional monsoon intensity (Ward et al., 2019; Wortham et al., 2017).

Forests in the Amazon region have expanded further in some areas over the past few decades due to fire suppression and/or agricultural land-abandonment (Rosan et al., 2019). Our data indicate that a natural trend of forest expansion and densification of savannas has occurred over a much longer time period, as predicted from feedbacks between increasing precipitation, decreasing fire disturbance, and increasing tree cover (Sternberg, 2001). Notably, woody vegetation expansion occurred despite increasing pre-Columbian human populations and associated disturbances (Souza et al., 2018) during the late Holocene. The genome-based population reconstructions in this regions show continuity of ancient peoples and practices beginning ~5,800 years before present with "a striking pattern of continuity with present-day people" beginning ~2,000 years ago (Posth et al., 2018)—i.e., the same period when speleothem isotope records suggest a shift towards wetter conditions due to increased monsoon intensity, although with major variability for local hydroclimates among surveyed sites (Ward et al., 2019).

From our map of vegetation change it is clear the dominant trend has been tree cover expansion and densification in both savanna and

forest ecosystems since the late Holocene, however, a few areas exist where vegetation remained relatively stable. Interestingly, transition zones did not show a consistent shift over time. This suggests that the woody vegetation expansion at forest–savanna boundaries might have been more strongly affected by disturbances (recent and old) at those sites. Humans are currently affecting vegetative cover in this region through land-use change and fire suppression, in some cases, and increasing the frequency of fire disturbance for rangeland expansion, in other cases (Andreoni & Londoño, 2019). Therefore, the long- and short-term drivers of woody vegetation expansion and current deforestation make the results from transition zones difficult to ascribe to a single process. For example, although woody vegetation expansion and densification appear to be the dominant response to climate variability over the past 1,600 years, a trend of decreasing tree coverage towards our easternmost sites also exists. Woody vegetation cover may have declined in this subregion due to the prevalence of dry deciduous or semideciduous tree species. Unlike evergreen tropical forests, deciduous or semideciduous dry forests in this subregion are adapted to low moisture of nutrient rich rock outcrops (Dexter et al., 2018). Under such conditions, increasing regional precipitation can decrease tree dominance and increase grass productivity, favoring the expansion of savannas (Silva et al., 2010).

Total carbon stocks did not vary consistently among ecosystem types, even though we found statistically significant differences between some forest and savannas due to a significant effect of soil order on carbon storage and outlier riparian zone profiles. The presence of gallery and riparian forests in our study region is contingent on soil moisture as well as soil nutrient inputs. During the mid-Holocene climatic conditions in South America shifted to becoming wetter (Marchant & Hooghiemstra, 2004) and shifts in the SASM intensity might have caused sediment and nutrient flows that favored forest expansion. In other regions, forest–savannas landscape mosaics can persist for millennia regardless of fluctuations in precipitation due to feedbacks that involve fire disturbance, nutrient limitation, and herbivore population density (Pausas & Bond, 2020). However, climate-driven increases in tree cover could still be recorded until the mid-1980s in open landscapes of central Brazil, even in sandy soils with low water retention capacity at the southeastern edge of the Amazon region (Marimon et al., 2006). In addition to hydrological feedbacks that favor increasing tree cover (Malhi et al., 2008), positive feedbacks between forest expansion and soil fertility would also be necessary to allow forest expansion because nutrient stoichiometries are fundamentally different between forests and savannas (Flores et al., 2019). Therefore, multiple factors must be considered to explain past and predict future woody vegetation expansion including climatic change, disturbances (e.g., floods and fires), and nutrient deposition from exogenous sources (e.g., atmospheric deposition and landscape translocation).

Most of the reconstructed increases in tree cover, evidenced here coincides with increasing density of pre-Columbian populations in southern Amazonia (estimated to vary between 500,000 and one million inhabitants from 1,250 to 1,500 AD (Souza et al., 2018). This

is important because it reveals that increasing pre-Columbian population densities apparently did not cause forest loss at the regional scales. Our findings are consistent with case studies of paleovegetation in other areas of the Amazon region (e.g., Lombardo et al., 2019; Silva, 2014; Smith & Mayle, 2018), but contradict a common assumption of human-driven expansion of open ecosystems in the region since the mid-Holocene. Recent anthropological findings could reconcile this apparent contradiction. Plant domestication dates back to >10,000 years ago in western Amazonia (Lombardo et al., 2020), however, the emergence of complex societies that relied on intensive land use in central Amazonia is much more recent (Capriles et al., 2019). Across the central and eastern Amazon basin human activity can be divided into three main phases: a precultivation period (>6,000 years ago); an early-cultivation period (6,000–2,500 years ago); and an intensive cultivation period (2,500–500 years ago; Maezumi et al., 2018). Our observation of increasing tree cover coincides with the chronology of intensification in sedentary settlements during the late Holocene, which probably resulted in an overall decline in deforestation and fire use across the region prior to European contact. On the other hand, current deforestation is interrupting a historical increase in tree cover in forests and savannas, which would have been further accelerated by the recent stimulation of tree growth due to increases in atmospheric CO_2 (Silva & Lambers, 2020). Moreover, current deforestation is also likely to change the regional climate by decreasing rainfall. Indeed, a recent increase in legal and illegal deforestation has followed the Brazilian Forest Act revision, with as of yet unquantified consequences for ecological and climatic stability (Freitas et al., 2018). Positive feedbacks between deforestation rates, warming climates, and declining precipitation could lead to a "deforestation-generated degradation of the hydrological cycle" (at 20%–25% deforestation threshold) beyond which large sections of the Amazon forest would be replaced with savannas unless major reforestation and conservation efforts can be implemented (Nobre & Lovejoy, 2018).

5 | CONCLUSION

Our data show a widespread process of woody vegetation expansion throughout the Amazon–Cerrado region since at least ~1,600 years prior to modern deforestation. We found evidence of increasing tree cover near forest–savanna ecotones as well as a significant densification of tree cover within most sampled forests and savannas with grass cover expanding only in a few locations characterized by dry climates and poorly developed soils. Several biophysical and biogeochemical mechanisms may have contributed to forest expansion and densification of woody vegetation in savannas, including positive feedbacks between tree cover and precipitation which can dampen fire disturbance and promote nutrient accumulation, which favor the persistence of closed canopies (Bomfim et al., 2019, 2020; Silva & Lambers, 2020). The observed expansion of forests into savannas could have significantly impacted carbon–water relations throughout the region, potentially affecting the balance between carbon sequestration,

evapotranspiration, and precipitation (Garcia et al., 2016). However, we did not observe a clear effect of changes in vegetation on soil carbon stocks. Future studies should focus on the mechanisms driving the permanence of carbon derived from woody vegetation expansion, informed by soil and climate records to improve predictions of rapidly changing ecosystem carbon-water balance. The next phase of understanding will come from the integration of plant, soil, and atmospheric data to understand the influence of human activity on ecosystem–climate feedbacks as a path towards improving carbon sequestration and water conservation.

DATA AVAILABILITY STATEMENT

The data used to produce all figures and tables presented here are available in Materials S1 and permanently stored and available at https://scholarsbank.uoregon.edu/.

ORCID

Jamie L. Wright https://orcid.org/0000-0001-6131-0078
Barbara Bomfim https://orcid.org/0000-0001-9510-2496
Lucas C. R. Silva https://orcid.org/0000-0002-4838-327X

REFERENCES

Abreu, R. C. R., Hoffmann, W. A., Vasconcelos, H. L., Pilon, N. A., Rossatto, D. R., & Durigan, G. (2017). The biodiversity cost of carbon sequestration in tropical savanna. *Science Advances*, *3*(8), 1–8. https://doi.org/10.1126/sciadv.1701284

Andreoni, M., & Londoño, E. (2019). Amid outrage over rainforest fires, many in the Amazon remain defiant. *The New York Times*.

AppEEARS Team. (2019). *Application for extracting and exploring analysis ready samples (AppEEARS)*. NASA EOSDIS Land Processes Distributed Active Archive Center (LP DAAC), USGS/Earth Resources Observation and Science (EROS) Center.

Austin, K. G., González-Roglich, M., Schaffer-Smith, D., Schwantes, A. M., & Swenson, J. J. (2017). Erratum: Trends in size of tropical deforestation events signal increasing dominance of industrial-scale drivers (2017 Environ. Res. Lett. 5 054009). *Environmental Research Letters*, *12*(7), 079601. https://doi.org/10.1088/1748-9326/aa7760

Behling, H. (1998). Late Quaternary vegetational and climatic changes in Brazil. *Review of Palaeobotany and Palynology*, *99*(2), 143–156. https://doi.org/10.1016/S0034-6667(97)00044-4

Berhe, A. A., Harden, J. W., Torn, M. S., Kleber, M., Burton, S. D., & Harte, J. (2012). Persistence of soil organic matter in eroding versus depositional landform positions. *Journal of Geophysical Research: Biogeosciences*, *117*, 1–16. https://doi.org/10.1029/2011JG001790

Bird, B. W., Abbott, M. B., Vuille, M., Rodbell, D. T., Stansell, N. D., & Rosenmeier, M. F. (2011). A 2,300-year-long annually resolved record of the South American summer monsoon from the Peruvian Andes. *Proceedings of the National Academy of Sciences of the United States of America*, *108*(21), 8583–8588. https://doi.org/10.1073/pnas.10037 19108

Bomfim, B., Silva, L. C. R., Doane, T. A., & Horwath, W. R. (2019). Interactive effects of land-use change and topography on asymbiotic nitrogen fixation in the Brazilian Atlantic Forest. *Biogeochemistry*, *142*(1), 137–153. https://doi.org/10.1007/s10533-018-0525-z

Bomfim, B., Silva, L. C. R., Marimon-Júnior, B. H., Marimon, B. S., Doane, T. A., & Horwath, W. R. (2020). Fire affects asymbiotic nitrogen fixation in southern Amazon forests. *Journal of Geophysical Research: Biogeosciences*, *125*(2). https://doi.org/10.1029/2019JG005383

Brannstrom, C., Jepson, W., Filippi, A. M., Redo, D., Xu, Z., & Ganesh, S. (2008). Land change in the Brazilian Savanna (Cerrado), 1986–2002: Comparative analysis and implications for land-use policy. *Land Use Policy*, *25*(4), 579–595. https://doi.org/10.1016/j.landu sepol.2007.11.008

Capriles, J. M., Lombardo, U., Maley, B., Zuna, C., Veit, H., & Kennett, D. J. (2019). Persistent Early to Middle Holocene tropical foraging in southwestern Amazonia. *Science Advances*, *5*(4), eaav5449. https://doi.org/10.1126/sciadv.aav5449

Cruz, F. W., Burns, S. J., Karmann, I., Sharp, W. D., Vuille, M., Cardoso, A. O., Ferrari, J. A., Dias, P. L. S., & Viana, O. (2005). Insolation-driven changes in atmospheric circulation over the past 116,000 years in subtropical Brazil. *Nature*, *434*, 63–65. https://doi.org/10.1029/2003JB002684

de Miranda, S. C., Bustamante, M., Palace, M., Hagen, S., Keller, M., & Ferreira, L. G. (2014). Regional variations in biomass distribution in Brazilian savanna woodland. *Biotropica*, *46*(2), 125–138. https://doi.org/10.1111/btp.12095

de Souza, J. G., Schaan, D. P., Robinson, M., Barbosa, A. D., Aragão, L. E. O. C., Marimon, B. H., Marimon, B. S., da Silva, I. B., Khan, S. S., Nakahara, F. R., & Iriarte, J. (2018). Pre-Columbian earth-builders settled along the entire southern rim of the Amazon. *Nature Communications*, *9*, 1125. https://doi.org/10.1038/s41467-018-03510-7

Dexter, K. G., Pennington, R. T., Oliveira-filho, A. T., Bueno, M. L., De Miranda, P. L. S., Neves, D. M., Osborne, C., Langan, L. J., & Dexter, K. G. (2018). Inserting tropical dry forests into the discussion on biome transitions in the tropics. *Frontiers in Ecology and Evolution*, *6*(July), 1–7. https://doi.org/10.3389/fevo.2018.00104

Didan, K. (2015). *MOD13A1 MODIS/Terra Vegetation Indices 16-day L3 global 500m SIN grid V006*. NASA EOSDIS Land Processes DAAC. https://doi.org/10.5067/MODIS/MOD13A1.006

Duarte-guardia, S., Peri, P. L., Amelung, W., Sheil, D., Laffan, S. W., Borchard, N., Bird, M. I., & Peri, P. L. (2019). Better estimates of soil carbon from geographical data: A revised global approach. *Mitigation and Adaptation Strategies for Global Change*, *24*, 355–372. https://doi.org/10.1007/s11027-018-9815-y

Elbasiouny, H., Abowaly, M., Abu-Alkheir, A., & Gad, A. A. (2014). Spatial variation of soil carbon and nitrogen pools by using ordinary Kriging method in an area of north Nile Delta, Egypt. *Catena*, *113*, 70–78. https://doi.org/10.1016/j.catena.2013.09.008

Elias, F., Hur, B., Junior, M., Júnior, F., Oliveira, M. D., Carlos, J., Oliveira, A. D., & Schwantes, B. (2019). Soil and topographic variation as a key factor driving the distribution of tree flora in the Amazonia/Cerrado transition. *Acta Oecologica*, *100*(July), 103467. https://doi.org/10.1016/j.actao.2019.103467

Flores, B. M., Staal, A., Jakovac, C. C., Hirota, M., Holmgren, M., & Oliveira, R. S. (2019). Soil erosion as a resilience drain in disturbed tropical forests. *Plant and Soil*, *450*(1-2), 11–25. https://doi.org/10.1007/s1110 4-019-04097-8

Frazer, G. W., Canham, C. D., & Lertzman, K. P. (1999). *Gap Light Analyzer (GLA), Version 2.0: Imaging software to extract canopy structure and gap light transmission indices from true-colour fisheye photographs, users manual and program documentation*. Simon Fraser University, Institute of Ecosystem Studies.

Freitas, F. L. M., Sparovek, G., Berndes, G., Persson, U. M., Englund, O., Barretto, A., & Mörtberg, B. (2018). Potential increase of legal deforestation in Brazilian Amazon after Forest Act revision. *Nature Sustainability*, *1*(11), 665–670. https://doi.org/10.1038/s41893-018-0171-4

Garcia, E. S., Swann, A. L. S., Villegas, J. C., Breshears, D. D., Law, D. J., Saleska, S. R., & Stark, S. C. (2016). Synergistic ecoclimate teleconnections from forest loss in different regions structure global ecological responses. *PLoS One*, *11*(11), 1–12. https://doi.org/10.1371/journal.pone.0165042

Hare, V. J., Loftus, E., Jeffrey, A., & Ramsey, C. B. (2018). Atmospheric CO_2 effect on stable carbon isotope composition of terrestrial fossil archives. *Nature Communications*, *9*. https://doi.org/10.1038/s41467-017-02691-x

Hoffmann, W. A., Geiger, E. L., Gotsch, S. G., Rossatto, D. R., Silva, L. C. R., Lau, O. L., Haridasan, M., & Franco, A. C. (2012). Ecological thresholds at the savanna-forest boundary: How plant traits, resources and fire govern the distribution of tropical biomes. *Ecology Letters*, *15*, 759–768. https://doi.org/10.1111/j.1461-0248.2012.01789.x

INMET. (2019). Brazilian Instituto Nacional De Meteorologia. Retrieved from https://portal.inmet.gov.br/

Kahle, D., & Wickham, H. (2013). ggmap: Spatial visualization with ggplot2. *The R Journal*, *5*(1), 144–161. https://doi.org/10.32614/RJ-2013-014

Krull, E. S., Bestland, E. A., & Gates, W. P. (2002). Soil organic matter decomposition and turnover in a tropical ultisol: Evidence from d13C, d15N and geochemistry. *Radiocarbon*, *44*, 93–112.

Ladd, B., Laffan, S. W., Amelung, W., Peri, P. L., Silva, L. C. R., Gervassi, P., Bonser, S. P., Navall, M., & Sheil, D. (2013). Estimates of soil carbon concentration in tropical and temperate forest and woodland from available GIS data on three continents. *Global Ecology and Biogeography*, *22*(4), 461–469. https://doi.org/10.1111/j.1466-8238.2012.00799.x

Ladd, B., Peri, P. L., Pepper, D. A., Silva, L. C. R., Sheil, D., Bonser, S. P., Laffan, S. W., Amelung, W., Ekblad, A., Eliasson, P., Bahamonde, H., Duarte-Guardia, S., & Bird, M. (2014). Carbon isotopic signatures of soil organic matter correlate with leaf area index across woody biomes. *Journal of Ecology*, *102*(6), 1606–1611. https://doi.org/10.1111/1365-2745.12309

Levy, M. C., Lopes, A. V., Cohn, A., Larsen, L. G., & Thompson, S. E. (2018). Land use change increases streamflow across the arc of deforestation in Brazil. *Geophysical Research Letters*, *45*(8), 3520–3530. https://doi.org/10.1002/2017GL076526

Lombardo, U., Iriarte, J., Hilbert, L., Ruiz-Pérez, J., Capriles, J. M., & Veit, H. (2020). Early Holocene crop cultivation and landscape modification in Amazonia. *Nature*, *581*(7807), 190–193. https://doi.org/10.1038/s41586-020-2162-7

Lombardo, U., Ruiz-pérez, J., Rodrigues, L., Mestrot, A., Mayle, F., Madella, M., Szidat, S., & Veit, H. (2019). Holocene land cover change in south-western Amazonia inferred from paleoflood archives. *Global and Planetary Change*, *174*, 105–114. https://doi.org/10.1016/j.glopl acha.2019.01.008

Maezumi, S. Y., Robinson, M., de Souza, J., Urrego, D. H., Schaan, D., Alves, D., & Iriarte, J. (2018). New insights from pre-Columbian land use and fire management in Amazonian dark earth forests. *Frontiers in Ecology and Evolution*, *6*(AUG), 111. https://doi.org/10.3389/fevo.2018.00111

Malhi, Y., Roberts, J. T., Betts, R. A., Killeen, T. J., Li, W., & Nobre, C. A. (2008). Climate change, deforestation, and the fate of the Amazon. *Science*, *319*(5860), 169–172. https://doi.org/10.1126/science.1146961

Marchant, R., & Hooghiemstra, H. (2004). Rapid environmental change in African and South American tropics around 4000 years before present: A review. *Earth-Science Reviews*, *66*, 217–260. https://doi.org/10.1016/j.earscirev.2004.01.003

Marimon, B. S., Lima, E. S., Duarte, T. G., & Chieregatto, L. C. (2006). Observations on the vegetation of northeastern Mato Grosso, Brazil.

IV. An analysis of the Cerrado-Amazonian Forest ecotone. *Edinburgh Journal of Botany*, *63*(2–3), 323–341. https://doi.org/10.1017/s0960428606000576

Nobre, C., & Lovejoy, T. E. (2018). Amazon tipping point. *Science Advances*, *4*(2), 1–2. https://doi.org/10.1126/sciadv.aat2340

Oliver, M. A., & Webster, R. (2014). Catena A tutorial guide to geostatistics: Computing and modelling variograms and kriging. *Catena*, *113*, 56–69. https://doi.org/10.1016/j.catena.2013.09.006

Parnell, A. (2020). *simmr: A stable isotope mixing model*. R package version 0.4.2. Retrieved from https://CRAN.R-project.org/package=simmr

Pausas, J. G., & Bond, W. J. (2020). Alternative biome states in terrestrial ecosystems. *Trends in Plant Science*, *25*(3), 250–263. https://doi.org/10.1016/j.tplants.2019.11.003

Posth, C., Nakatsuka, N., Lazaridis, I., Skoglund, P., Mallick, S., Lamnidis, T. C., Rohland, N., Nägele, K., Adamski, N., Bertolini, E., Broomandkhoshbacht, N., Cooper, A., Culleton, B. J., Ferraz, T., Ferry, M., Furtwängler, A., Haak, W., Harkins, K., Harper, T. K., … Reich, D. (2018). Reconstructing the deep population history of Central and South America. *Cell*, *175*, 1185–1197. https://doi.org/10.1016/j.cell.2018.10.027

Rosan, T. M., Aragão, L. E. O. C., Oliveras, I., Phillips, O. L., Malhi, Y., Gloor, E., & Wagner, F. H. (2019). Extensive 21st-century woody encroachment in South America's savanna. *Geophysical Research Letters*, *46*(12), 6594–6603. https://doi.org/10.1029/2019GL082327

Sanaiotti, T. M., Martinelli, L. A., Victoria, R. L., Trumbore, S. E., & Camargo, P. B. (2002). Past vegetation changes in Amazon savannas determined using carbon isotopes of soil organic matter. *Biotropica*, *34*(1), 2. https://doi.org/10.1646/0006-3606(2002)034[0002:PVCIAS]2.0.CO;2

Sande, M. T., Gosling, W., Correa-Metrio, A., Prado-Junior, J., Poorter, L., Oliveira, R. S., Mazzei, L., & Bush, M. B. (2019). A 7000-year history of changing plant trait composition in an Amazonian landscape; the role of humans and climate. *Ecology Letters*, *22*(6), 925–935. https://doi.org/10.1111/ele.13251

Santos, G. M., Southon, J. R., Drenzek, N. J., Ziolkowski, L. A., Druffel, E., Xu, X., Zhang, D., Trumbore, S., Eglinton, T. I., & Hughen, K. A. (2019). Blank assessment for ultra-small radiocarbon samples: Chemical extraction and separation versus AMS. *Radiocarbon*, *52*(2), 1322–1335. https://doi.org/10.1017/s0033822200046415

Schmidt, M. W. I., Torn, M. S., Abiven, S., Dittmar, T., Guggenberger, G., Janssens, I. A., Kleber, M., Kögel-Knabner, I., Lehmann, J., Manning, D. A. C., Nannipieri, P., Rasse, D. P., Weiner, S., & Trumbore, S. E. (2011). Persistence of soil organic matter as an ecosystem property. *Nature*, *478*(7367), 49–56. https://doi.org/10.1038/nature10386

Silva, L. C. R. (2014). Importance of climate-driven forest – Savanna biome shifts in anthropological and ecological research. *Proceedings of the National Academy of Sciences of the United States of America*, *111*(37), E3831–E3832. https://doi.org/10.1073/pnas.1413205111

Silva, L. C. R. (2017). Carbon sequestration beyond tree longevity. *Science*, *355*(6330), 1141. https://doi.org/10.1126/science.aan0109

Silva, L. C. R., Doane, T. A., Corrêa, R. S., Valverde, V., Pereira, E. I. P., & Horwath, W. R. (2015). Iron-mediated stabilization of soil carbon amplifies the benefits of ecological restoration in degraded lands. *Ecological Applications*, *25*(5), 1226–1234. https://doi.org/10.1890/14-2151.1

Silva, L. C. R., Haridasan, M., Sternberg, L., Franco, A. C., & Hoffmann, W. A. (2010). Not all forests are expanding over central Brazilian savannas. *Plant and Soil*, *333*(1–2), 431–442. https://doi.org/10.1007/s11104-010-0358-6

Silva, L. C. R., Hoffmann, W. A., Rossatto, D. R., Franco, A. C., Horwath, W. R., Plant, S., December, N., Haridasan, M., Franco, A. C., & Horwath, W. R. (2013). Can savannas become forests? A coupled analysis of nutrient stocks and fire thresholds in central Brazil. *Plant and Soil*, *373*(1), 829–842. https://doi.org/10.1007/s11104-013-1822-x

Silva, L. C. R., & Lambers, H. (2018). Soil-plant-atmosphere interactions: Ecological and biogeographical considerations for climate-change research. In W. R. Horwath & Y. Kuzyakov (Eds.), *Climate change impacts on soil processes and ecosystem properties* (pp. 29–60).

Silva, L. C. R., & Lambers, H. (2020). Soil-plant-atmosphere interactions: Structure, function, and predictive scaling for climate change mitigation. *Plant and Soil*, 1–23. https://doi.org/10.1007/s11104-020-04427-1

Silva, L. C. R., Sternberg, L., Haridasan, M., Hoffmann, W. A., Miralles-Wilhelm, F., & Franco, A. C. (2008). Expansion of gallery forests into central Brazilian savannas. *Global Change Biology*, *14*(9), 2108–2118. https://doi.org/10.1111/j.1365-2486.2008.01637.x

Smith, R. J., & Mayle, F. E. (2018). Impact of mid- to late Holocene precipitation changes on vegetation across lowland tropical South America: A paleo-data synthesis. *Quaternary Research*, *89*, 134–155. https://doi.org/10.1017/qua.2017.89

Smith, T., & Smith, R. (2015). *Elements of ecology* (9th ed.). Pearson.

Soil Survey Staff. (2014). *Keys to soil taxonomy* (12th ed.). USDA-Natural Resources Conservation Service.

Spracklen, D. V., Arnold, S. R., & Taylor, C. M. (2012). Observations of increased tropical rainfall preceded by air passage over forests. *Nature*, *489*(7415), 282–285. https://doi.org/10.1038/nature11390

Staal, A., Tuinenburg, O. A., Bosmans, J. H. C., Holmgren, M., Van Nes, E. H., Scheffer, M., Zemp, D. C., & Dekker, S. C. (2018). Forest-rainfall cascades buffer against drought across the Amazon. *Nature Climate Change*, *8*(6), 539–543. https://doi.org/10.1038/s41558-018-0177-y

Sternberg, L. (2001). Savanna-forest hysteresis in the tropics. *Global Ecology and Biogeography*, *10*(4), 369–378. https://doi.org/10.1046/j.1466-822X.2001.00243.x

Trumbore, S. (2000). Age of soil organic matter and soil respiration: Radiocarbon constraints on belowground C dynamics. *Ecological Applications*, *10*(2), 399–411. https://doi.org/10.1890/1051-0761(2000)010[0399:AOSOMA]2.0.CO;2

Trumbore, S. (2009). Radiocarbon and soil carbon dynamics. *Annual Review of Earth and Planetary Sciences*, *37*, 47–66. https://doi.org/10.1146/annurev.earth.36.031207.124300

Veldman, J. W., Overbeck, G. E., Negreiros, D., Mahy, G., Le Stradic, S., Fernandes, G. W., Durigan, G., Buisson, E., Putz, F. E., & Bond, W. J. (2015). Where tree planting and forest expansion are bad for biodiversity and ecosystem services. *BioScience*, *65*(10), 1011–1018. https://doi.org/10.1093/biosci/biv118

Victoria, R. L., Fernandes, F., Martinelli, L. A., Cassia Piccolo, M., Camargo, P. B., & Trumbore, S. (1995). Past vegetation changes in the Brazilian Pantanal arboreal-grassy savanna ecotone by using carbon isotopes in the soil organic matter. *Global Change Biology*, *1*(3), 165–171. https://doi.org/10.1111/j.1365-2486.1995.tb00018.x

von Fischer, J. C., Tieszen, L. L., & Schimel, D. S. (2008). Climate controls on C_3 vs. C_4 productivity in North American grasslands from carbon isotope composition of soil organic matter. *Global Change Biology*, *14*(5), 1141–1155. https://doi.org/10.1111/j.1365-2486.2008.01552.x

Vuille, M., Burns, S. J., Taylor, B. L., Cruz, F. W., Bird, B. W., Abbott, M. B., Kanner, L. C., Cheng, H., & Novello, V. F. (2012). A review of the South American monsoon history as recorded in stable isotopic proxies over the past two millennia. *Climate of the Past*, *8*(4), 1309–1321. https://doi.org/10.5194/cp-8-1309-2012

Ward, B. M., Wong, C. I., Novello, V. F., Mcgee, D., Santos, R. V., Silva, L. C. R., Cruz, F. W., Wang, X., Edwards, R. L., & Cheng, H. (2019). Reconstruction of Holocene coupling between the South American Monsoon System and local moisture variability from speleothem $\delta^{18}O$ and $^{87}Sr/^{86}Sr$ records. *Quaternary Science Reviews*, *210*, 51–63. https://doi.org/10.1016/j.quascirev.2019.02.019

Wortham, B. E., Wong, C. I., Silva, L. C. R., McGee, D., Montañez, I. P., Troy Rasbury, E., Cooper, K. M., Sharp, W. D., Glessner, J. J. G., & Santos, R. V. (2017). Assessing response of local moisture conditions in central Brazil to variability in regional monsoon intensity using speleothem $^{87}Sr/^{86}Sr$ values. *Earth and Planetary Science Letters*, *463*, 310–322. https://doi.org/10.1016/j.epsl.2017.01.034

Zemp, D. C., Schleussner, C., Barbosa, H. M. J., Hirota, M., Montade, V., Sampaio, G., Staal, A., Wang-Erlandsson, L., & Rammig, A. (2017).

Self-amplified Amazon forest loss due to vegetation-atmosphere feedbacks. *Nature Communications*, *8*, 1–10. https://doi.org/10.1038/ncomms14681

SUPPORTING INFORMATION

Additional supporting information may be found online in the Supporting Information section.